Sanitized Copy Approved for Release 2011/03/07 : CIA-RDP80T00246A014400530001-3

INFORMATION REPORT INFORMATION REPORT

EXPEDITE

CENTRAL INTELLIGENCE AGENCY

This material contains information affecting the National Defense of the United States within the meaning of the Espionage Laws, Title 18, U.S.C. Secs. 793 and 794, the transmission or revelation of which in any manner to an unauthorized person is prohibited by law.

C-O-N-F-I-D-E-N-T-I-A-L

50X1-HUM

COUNTRY USSR

REPORT [redacted]

SUBJECT [redacted] A. I. Leipunsky's "Physical Characteristics of Reactor BR-V" [redacted]

[redacted]

(Description, technical data on power reactors)

DATE DISTR. 6 Nov 61 50X1-HUM

NO. PAGES 1 50X1-HUM

REFERENCES [redacted]

DATE OF INFO. [redacted]

PLACE & DATE ACQ. [redacted]

50X1-HUM

THIS IS UNEVALUATED INFO[redacted]

[redacted]

-end-

C-O-N-F-I-D-E-N-T-I-A-L

STATE		ARMY		NAVY		AIR		FBI		AEC					

INFORMATION REPORT INFORMATION REPORT

NOFORN NO DISSEM ABROAD LIMITED

LIMITED: Dissemination limited to full-time employees of CIA, AEC and FBI; and, within State and Defense, to the intelligence components, other offices producing NIS elements, and higher echlons with their immediate supporting staffs. Not to be disseminated to consultants, external projects or reserve personnel on short term active duty (excepting individuals who are normally full-time employees of CIA, AEC, FBI, State or Defense) unless the written permission of the originating office has been obtained through the Assistant Director for Central Reference, CIA.

Sanitized Copy Approved for Release 2011/03/07 : CIA-RDP80T00246A014400530001-3

Sanitized Copy Approved for Release 2011/03/07 : CIA-RDP80T00246A014400530001-3

50X1-HUM

Page Denied

Next 1 Page(s) In Document Denied

Sanitized Copy Approved for Release 2011/03/07 : CIA-RDP80T00246A014400530001-3

Sanitized Copy Approved for Release 2011/03/07 : CIA-RDP80T00246A014400530001-3

PHYSICAL CHARACTERISTICS OF REACTOR BR-V

50X1-HUM

Introduction

Reactor BR-V is a fast neutron research reactor with 5 Mw thermal power designed for the purposes of gaining experience and gathering data necessary for the construction of fast neutron breeder reactors for power production. Plutonium oxide is used for fuel. Sodium is used as coolant. The reflector consists of two layers - a thin layer of natural U and thick layer of Ni.

A detailed account of the construction of this reactor was given at the Second International Conference for Peaceful Uses of Atomic Energy.[1] In the reactor there are large amounts of equipment designed for experiments with fast, intermediate and slow neutrons. The experiments deal with technology physics and characteristics of materials. Large numbers of powerful neutron beams, experimental holes, and thermal columns provide broad possibilities for determination of nuclear constants necessary for reactor calculations and for conducting work in nuclear physics.

Longitudinal and transverse sections of the reactor are shown in Figures 1 and 2. Channels designed for conducting loop experiments run along the vertical axis of the core. At a distance of 40 cm from the center of the reactor, vertical channels 70 mm across run through the Ni reflector. (OK-70). Two channels for fast neutrons run horizontally from the edge of the core through the reflector and shielding (B-1 and B-3). Channel B-2, awide running out horizontally from the Ni reflector is for a beam of neutrons of intermediate energy, as well as for experiments on radiation shielding. The reactor has a graphite thermal column

Sanitized Copy Approved for Release 2011/03/07 : CIA-RDP80T00246A014400530001-3

Sanitized Copy Approved for Release 2011/03/07 : CIA-RDP80T00246A014400530001-3

having an aggregation of vertical channels 20 mm across, not to mention channels OK-3 and AK, 70 mm and 100 mm across, respectively.

The physical characteristics of reactor BR-V that have been measured are presented in this paper.

Neutron Distribution

The energy spectrum of neutrons is different in different parts of reactor BR-V. In the core of the reactor the neutron spectrum is rather hard; a considerable part of the spectrum lies above 100 Kev. Going through the Ni reflector, the neutrons quickly lose their energy in inelastic and elastic collisions so that in the outer layers of the reflector the energy of the neutron spectrum is no more than a few 10's of electron volts.

The fluctuation of the neutron spectrum, especially in the kilovolt energy range, presents very difficult experimental problems. For this reason, details of the spectrum were obtained only in the region of relatively fast neutrons ($E_n > 50$ Kev) for the most important neutron beams and channels.

In the rest of the cases, cross-sections of reactions with known energy dependence, averaged over the energy of the experimental spectrum, were used as characteristics of the spectra. For these detectors were used the reactions U-238 (n,f), Th-232 (n,f) and Al-27 (n,α) Na-24, having effecting thresholds about 1, 4 and 5 Mev, respectively and approximately constant cross-section above the threshold, the reaction Pu-239 (n,f), a cross-section which is almost constant in the region from 50 Kev to 6 Mev and the reactions Na-23(n,γ), Cu-63 (n,γ) and Au-197 (n,γ) which are slow neutron detectors.

In order to get the best value for the moderation of the neutron spectrum in the reflector, the fission reaction of U-235 is used as well as the Pu-239 (n,f).

Sanitized Copy Approved for Release 2011/03/07 : CIA-RDP80T00246A014400530001-3

Sanitized Copy Approved for Release 2011/03/07 : CIA-RDP80T00246A014400530001-3

The U-235 fission reaction has a cross-section with greater energy dependence in the slow region. To get further information about the soft part of the spectrum in the reflector of the reactor, research was done on the spacial distribution of neutrons with $E_n \approx 5$ ev., using Au-197 - the self shielding method.[2]

These detectors were exposed in the vertical experimental channel, located at a distance of 5 cm from the center of the reactor. Small fission chambers, containing thin layers of fissionable material were used as fission detectors. The chambers were filled with pure argon under a pressure of 10 atmospheres. The method of filling assured that the chambers would be independent of time and temperature up to 400°C, with an accuracy of 2%, which seemed entirely sufficient, since the temperature of the core had been shown by measurement not to exceed 250°C.

The activation detectors were in the form of foils of Al, Cu and Au and tablets of NaF. β activity was measured with a Geiger counter, the sample being placed at the end of the counter. The total flux of neutrons of all energy was measured only in those places in the reactor where the principal part of the neutron spectrum lay in the energy region in which the cross-section of the fission of Pu-239 is constant. In this case, a fission chamber with Pu-239 acts as a detector for all energies by the following equation:

$$N_g = n_g \eta \sigma_f \phi$$

n_g = the number of Pu-239 nuclei in the fission chamber

η = effectiveness with which the fissions are detected

ϕ = total flux of neutrons

σ_f = fission cross-section of Pu-239

Sanitized Copy Approved for Release 2011/03/07 : CIA-RDP80T00246A014400530001-3

Sanitized Copy Approved for Release 2011/03/07 : CIA-RDP80T00246A014400530001-3

n_g was determined from the α activity of the layer of Pu-239 in the chamber. Similarly the fast neutron flux was determined with fission counters using natural and depleted U. The amounts of material in these chambers were determined by comparing the number of counts from these chambers with the number of counts from Pu-239 fission chambers, exposed to the same beam of slow neutrons. The direct measurements of the neutron spectrum were conducted in the vertical channel OK-70. (See Fig. 1 and 2).

In channel OK-70 the spectrum of neutrons was measured in an ionization chamber filled with a mixture of He^3 and argon. In channel B-3 the spectrum of neutrons was determined by passing through a hydrogen-containing substance, n-Hexane, in good geometry. As a detector a boron counter was used.

The transmission curve was subjected to an inverse LaPlace transformation. The derived "original" gave the neutron spectrum, after the energy sensitivity of the detector and the variation with energy of the total cross-section of H and C contained in the scatterer were taken into account.

The spectrum of neutrons in channel B-3 was also measured with photo emulsions. These results were the lowest ones obtained. In Fig. 3 is given the counting rate of the different detectors along the vertical axis of the reactor. The edge of the core is represented by the dotted line. In the central region of the core all of the curves, even those showing the number and distribution of fissions of Th-232 and of capture in Au-197, which have completely different dependence of cross-section on energy, obey the same law. This shows that for a large enough core and in those regions that are sufficiently far from the boundaries, the energy spectrum of neutrons is constant. In this region the reflector has no effect. In the peripheral layers of the core, the effect of the flux of slow neutrons coming from the reflector begins to show up. As a result, in these regions

Sanitized Copy Approved for Release 2011/03/07 : CIA-RDP80T00246A014400530001-3

Sanitized Copy Approved for Release 2011/03/07 : CIA-RDP80T00246A014400530001-3

distributions recorded with detectors having different energy sensitivity behave differently. This difference appears most strongly in the reflector of the reactor where the neutrons quickly lose their energy as a result of inelastic scattering after which they continue to slow down by elastic scattering. Owing to the strong blocking of resonance capture by resonance scattering the probability of escaping resonance capture by slowing down elastically in Ni is sufficiently great that the greater part of the neutrons pass through the resonance region in Ni uncaptured and continue to be slowed down without appreciable absorption to energies of the order of 10 ev, where the $^1/v$ law begins to become important. The qualitative picture described explains the fact that the rate of neutron capture in Au increases in the reflector to almost three times its value in the center of the core, in spite of strong self shielding in the foils from lower resonances. The sharp increase in cross-section in passing from the core to the reflector appears also in the distribution of fissions in U-235 and, to a lesser extent, in Pu-239. The Pu-239 fission cross-section is less energy dependent than the others involved.

In Figure 4 is given distributions of reaction rate of Al-27(nα) and of capture in Na-23, Cu-63 and Au-197 (thin indicators) measured in the experimental vertical channel located 5 cm from the center of the reactor. These results confirmed conclusions reached on the basis of examination of data obtained from the central channel of the reactor. The distributions of specific activities of the Au foils, enclosed on both sides with Au filters of different thicknesses, characterize the strong moderation of neutrons in the Ni reflector. By extrapolation of these data to 0 thickness of indicator foil and infinite thickness of filter, it is possible to get the activity dependent only on neutrons with energy in the region of the resonance E_n = 4.9 ev. In Figure 5 is presented distributions of activity

Sanitized Copy Approved for Release 2011/03/07 : CIA-RDP80T00246A014400530001-3

Sanitized Copy Approved for Release 2011/03/07 : CIA-RDP80T00246A014400530001-3

of indicators without filters and with filters of different thicknesses and distributions received by means of extrapolation. In Fig. 6 is represented the spacial distribution of neutron flux with En = 4.9 ev along the height of the experimental channel, computed from the extrapolated activity for the rated output of the reactor.

In contrast to the distributions recorded with detectors sensitive to slow neutrons, the distributions Th-232 (n,f) and Al(n,α) show a sharp drop in the reflector of the reactor, which was to be expected inasmuch as the fast neutrons quickly reduce their energy by elastic scattering in the Ni below the thresholds for these reactions.

The curves in Fig. 3 are plotted in relative units. For normalization it is necessary to know the cross-section of the corresponding reaction in the center of the core of the reactor.

In the center of the core, the ratio between the fission cross-section of Pu-239 and the fission cross-sections of U-235, U-238 and the capture cross-section in Au-197, respectively were measured. Results received are plotted in the first column of Table I.

The neutron flux could be determined only in those parts of the reactor where the principal part of the neutrons lay in the energy range for which the cross-section of Pu-239 (n,f) is constant, or in the thermal region. In the reflector of the reactor and in the beams emerging from the reflector the neutron spectrum lies in the resonance region, where the cross-section of Pu-239 (n,f) shows strong fluctuations; therefore, the neutron flux cannot be obtained for these regions by the method used.

A summary of the data concerning the flux is given in Table 2. The

Sanitized Copy Approved for Release 2011/03/07 : CIA-RDP80T00246A014400530001-3

Sanitized Copy Approved for Release 2011/03/07 : CIA-RDP80T00246A014400530001-3

distribution of thermal flux and of cadmium ratio along the axis of the thermal column was measured by means of radioactive detectors of Au-197, In-115 and Cu-63. The curve in Fig. 7 shows the average values of the data measuring the slow neutron flux, normalized to the values obtained for channel AK. The cadmium ratio was corrected for the $^1/v$ sensitivity of the detector.

Fig. 8 and 9 show the neutron spectrum in B-3, coming from the edge of the core, obtained by analysis of a transmission curve through an H-containing medium and by using photo emulsions. The first maximum in this spectrum, lying at low energy is from neutrons slowed down in the reflector.
The one at higher energy, 2.5 Mev, corresponds to the spectrum of fission neutrons. The spectrum of neutrons in channel OK-70, measured with chambers containing He^3 is shown in Fig. 10.

Normalized values of the above flux pertain to a power of 5 Mw, taking into account fissions in U-235 and U-238 blanket elements. The power was estimated from the counting rates of Pu-239 fission chambers, having known amounts of material, corrected for the non-uniformity of the distribution of fissions over the core. In addition the power was checked, at the rated value, the highest power of the reactor, by taking a heat balance.

Quantitative calculation of spacial-energy distributions of neutrons in reactor BR-V were carried out using 9 and 18 groups. The neutron distribution obtained for the 9 group calculation by means of Carlson's S_4 approximation for the solution of the Boltzmann equation agreed satisfactorily with the experimental curve obtained with Pu-239, U-238 and activated gold in the core. (See Table 1) This attests to the accuracy of the calculation of the spectrum in the core, presented in Fig. 11. The neutron spectrum measured in the range 0.1 - 1.2 Mev

Sanitized Copy Approved for Release 2011/03/07 : CIA-RDP80T00246A014400530001-3

Sanitized Copy Approved for Release 2011/03/07 : CIA-RDP80T00246A014400530001-3

in channel OK-70 also is in satisfactory agreement with calculations. However, the experimental curves for fission of Pu-239, U-235 and for activation of Au in the reflector show poor correlation with theoretical curves. While the theoretical curve of activation of Au drops off in the reflector, the experimental curve shows a sharp maximum. As a consequence, a calculation of the spacial-energy distribution of neutrons was made using an 18 group approximation for a spherical model reactor. These calculations resulted in better agreement with experiment, as is illustrated in Fig. 12, where theoretical and experimental Au activation curves are compared. In spite of the obvious improvement, there is not complete agreement between calculation and experiment. The apparent cause of this divergence is that the assumption of a spherical, homogenious system is very far from the actual construction of the reactor. Exact calculation of the effects of construction details (the annular shape, the boundary of the reflector, etc.) present difficult problems. It is possible also that the constants of the system used in the calculation were not absolutely accurately selected. It should be pointed out, however, that an independent study of the spacial-energy distribution in Ni (4) gave satisfactory agreement with the calculated results.

Continuous bombardment of U in the reactor permits measurement of

$\alpha = \frac{\overline{\sigma}_c}{\overline{\sigma}_f}$, the ratio of the average radiative capture cross-section to the average fission cross-section, a characteristic that determines to a large extent the rate of breeding. For this measurement, one of the U rods in the blanket having been exposed to a neutron flux of 6.3×10^{21} n/cm^2 was subjected to radio-chemical treatment. By measuring the concentration of Pu-239 in Uranium (from the specific α activity) and the concentration of Pu-240 in plutonium (by counting spontaneous fissions) the ratio of the average radiative capture cross-sections in Pu-239

Sanitized Copy Approved for Release 2011/03/07 : CIA-RDP80T00246A014400530001-3

Sanitized Copy Approved for Release 2011/03/07 : CIA-RDP80T00246A014400530001-3

and U-238 was determined. The value of this quantity, averaged over the length of the rod was 1.85 ± 0.2, which is in satisfactory agreement with the result of the calculation for the 18th neutron group - 1.95. The ratio, α, computed from the experimental data and the calculations, is $\alpha = 0.19 \pm 0.01$.

Some Peculiarities of Kinetics and Measurements of Perturbations

For a research reactor, one of the most important problems is that of the safe operation of the reactor. A substantial role in the question is played by power effects, that is, the influence of changes in power on the reactivity. The origin of the power effects in a fast reactor are connected, for the most part, with the heating and expansion of elements in the core and reflector of the reactor. Inhomogeneous heating and differing coefficients of thermal expansion cause these elements to shift relative to each other and to deform. Expansion connected with homogeneous heating and corresponding changes in reactivity usually determine the temperature coefficient. Conditions of uniform heating develop in the elevated temperature of Na at the intake; the corresponding temperature coefficient in BR-V is equal to:

$$\alpha_t = -2.8 \times 10^{-5}/^{\circ}C$$

The change in form of the core, connected with inhomogeneous heating from heat evolved in the reactor, with constant temperature of Na at the intake, and corresponding changes in reactivity characterize the asymptotic power coefficient. In BR-V this coefficient equals:

$$\alpha_M = -2 \times 10^{-4}/Mw$$

The change in reactivity caused by a given change in power is not immediately determined. The nature of such a transitory approach to asymptotic power and

Sanitized Copy Approved for Release 2011/03/07 : CIA-RDP80T00246A014400530001-3

Sanitized Copy Approved for Release 2011/03/07 : CIA-RDP80T00246A014400530001-3

temperature conditions plays a very large role in the problem of stable operation of the reactor. The overall relation between reactivity and power, with computation of additional surface effects is represented in Figure 13. The investigation of the power effect in BR-V was for the purpose of getting information about the nature of the relationship between reactivity and power.

If one denotes power as a function of reactivity by the symbol $m(\rho)$ and reactivity as a function of power by $\rho(M)$ then the reactor may be represented (see Fig. 14) as a quadripole with inverse coupling (with the uncoupled system AR* and the constant condition of operation of the heat exchanger) with the function $M(\rho)$, power in terms of effects of reactivity.

By analogy one may apply methods derived for electrical systems to the reactor as well. For analysis of electrical amplifier, two methods are widely used:

1. The method of harmonic analysis. That is, of frequency-phase characteristics of the outgoing parameter in the presence of sinusoidal fluctuation of the incoming parameter at various frequencies.
2. Impulse method. That is, observing the reaction of the outgoing parameter in the presence of intermittent fluctuations of the incoming one.

By the first method the transfer function $M_0(j\omega)$ is measured. This is the ratio of the complex amplitude of the fluctuation in power to the complex amplitude of the fluctuation in reactivity. When measurements are made at low power the influence of power on reactivity is small (the effect of power on reactivity is proportioned to the absolute value of the fluctuation - not the % fluctuation) and the transfer function becomes $m_0(j\omega)$.

*Automatic Regulating System

Sanitized Copy Approved for Release 2011/03/07 : CIA-RDP80T00246A014400530001-3

Sanitized Copy Approved for Release 2011/03/07 : CIA-RDP80T00246A014400530001-3

If one designates by $\overline{M}\rho_o(j\omega)$ the open loop transfer function ($\overline{M}$ - the average value of power, $\rho(j\omega)$ - power coefficient of reactivity), then according to the theory of systems with inverse feedback

$$Mo(j\omega) = \frac{mo(j\omega)}{1-\overline{M}\rho_o(j\omega)mo(j\omega)}$$

Hence
$$\overline{M}\rho_o(j\omega) = \frac{1}{mo(j\omega)} - \frac{1}{Mo(j\omega)}$$

Measurements taken at 0 power and at some powers other than 0 in principle allow calculation of the transfer function for any power. An experimental study of $mo(j\omega)$ and $Mo(j\omega)$ was extensively used, for example in reactor EBR-I.[5]

The second method, applied to a reactor, consists of intermittently changing the reactivity and then watching the transient processes of change in power $M_1(t)$ and $m_1(t)$.

In principle, both methods are equivalent inasmuch as the observed functions are linked.[6]

$$Mo(j_\omega) = j\omega\int_0^\infty M_1(t)e^{-j\omega t}\,dt$$

$$mo(j_\omega) = j\omega\int_0^\infty m_1(t)e^{-j\omega t}\,dt$$

$$M_1(t) = \frac{1}{2\pi}\int_{\sigma-j\omega}^{\sigma+j\omega}\frac{Mo(j\omega)}{j\omega}\;e^{-j\omega}\,d\omega$$

$$m_1(t) = \frac{1}{2\pi}\int_{\sigma-j\omega}^{\sigma+j\omega}\frac{Mo(j\omega)}{j\omega}\;e^{-j\omega}\,d\omega$$

Sanitized Copy Approved for Release 2011/03/07 : CIA-RDP80T00246A014400530001-3

Sanitized Copy Approved for Release 2011/03/07 : CIA-RDP80T00246A014400530001-3

in EBR-I experiments were carried out with $M_1(t)$ fixed.

It is possible to use a variation of this method, that is, to observe the change in reactivity corresponding to an intermittent change in inpower (incoming and outgoing parameters of the quadripole change places).

Let the corresponding functions become:

$Ro(j\omega)$	transfer functions of power for
$\eta o(j\omega)$	sufficiently small power
$R_1(t)$	transient characteristics i.e., changes in reactivity
$\eta_1(t)$	corresponding to intermittent changes in power
$\rho o(j\omega)$	transfer function and transient characteristic of the chain
$\rho_1(j\omega)$	of inverse feedback

$$Ro(j\omega) = j\omega \int_0^\infty R_1(t)e^{-j\omega t}\, dt$$

and analogously for $\eta o(j\omega$, $R_1(t)$ and $\eta_1(t)$

From which $$Ro(j\omega) = \frac{1}{Mo(j\omega)},\quad \eta o(j\omega) = \frac{1}{mo(j\omega)}$$

The transient characteristic of dependence of reactivity on power is directly obtained as the difference of two measured functions:

$$\overline{M}\,\rho_1(t) = \eta_1(t) - R_1(t)$$

This method was used in the investigation of BR-V.

Obviously from the relationships that have been given, each of these methods is equivalent in principle, but practical considerations make each method

Sanitized Copy Approved for Release 2011/03/07 : CIA-RDP80T00246A014400530001-3

Sanitized Copy Approved for Release 2011/03/07 : CIA-RDP80T00246A014400530001-3

suited for answering one question and limited for another.

1. The frequency - phase characteristic may be obtained with greater accuracy than transient characteristics.
2. From the frequency-phase characteristic, the frequency and limits of power may be determined, from which sustained and increasing oscillations of power may be obtained.
3. The transient characteristics may be used most directly for calculations of properties of the reactor when it is not operating at steady power (inasmuch as time functions are directly involved here). If transfer functions are used for these purposes, difficulties of transformation arise, which result in poorer accuracy because of the approximations that must be used.
4. The last method of inquiry uses the system of automatic controls which provide the change in reactivity necessary for intermittent changes in power. Using system AR is advantageous since any condition can be studied there in safety. The example of the melting of the core of EBR-I shows that this must not be disregarded.
5. The inertial characteristics of system AR limit its use for investigation of processes that take place sufficiently rapidly.

During the experiments the power fluctuated intermittently. The fluctuation amounted to 5 - 20% of the original value. The system AR provided a fluctuation of power with time of 0.3 sec.

From the position of the Selsyn operated automatic recorder, it was obvious that the accuracy of reproduction of the result on the reactivity was 5×10^{-5}%. The inertia of the indicator and the automatic recorder does not

Sanitized Copy Approved for Release 2011/03/07 : CIA-RDP80T00246A014400530001-3

Sanitized Copy Approved for Release 2011/03/07 : CIA-RDP80T00246A014400530001-3

allow the functions $R_1(t)$ and $\eta_1(t)$ to be obtained for the interval of time from 0 to 3-5 sec. after a change in power. Now we can give a graphic physical explanation for the relationship $\overline{M} \cdot \rho_1(t) = \eta_1(t) - R_1(t)$.

The position of the regulator $\eta_1(t)$ allows that change in reactivity which is necessary for an almost intermittent change in power. It is obvious that at high power as well, for the same relative change in power, it is necessary to have a similar change in the multiplication coefficient. The new position of the regulator $R(t)$ indicates that part of the change in reactivity which depends on power.

The most interesting cases of curves $R^{\cdot}(t)$ and $\rho_1(t)$ are presented in the series of Figures 15, 16, 17 where 1 cm **AR** amounts to 2×10^{-5} units of reactivity. Fig. 15 represents the normal operating condition, with the rod at first position.* The power effect is absent for 25 sec. and then becomes negative. The negative effect is connected with the arrival at the reactor intake of heated Na which has made a complete circuit through the reactor. It should be noted that after a jump in power, a temperature equilibrium is reached. Fig. 16 depicts the characteristics of the operating conditions that exist then. **A** clearly discernible positive effect occurs after 30 sec. Fig. 17 gives the characteristic conditions with natural circulation - the power effect is positive at all times observed (up to 3 min.) although it decreases after a maximum at 30-40 sec.

Thus the method described above allows one to get the transient characteristics of the influence of power on reactivity in operating conditions, whereas without system **AR** an unstable situation would result from such experiments and the investigation could not easily be carried out in any other way.

---

*This apparently refers to startup.

Sanitized Copy Approved for Release 2011/03/07 : CIA-RDP80T00246A014400530001-3

Sanitized Copy Approved for Release 2011/03/07 : CIA-RDP80T00246A014400530001-3

At present, work on investigation of power effects and of their nature continues. Besides studies of kinetics the following other investigations were carried out in BR-V in sub-critical and critical states:

Measurements of change in reactivity (1) with movement of control rod;

(2) when the core is filled with Na.

(3) when a single fuel element is extracted.

(4) when certain samples are moved through a loop channel.

Some results of these measurements are presented in Fig. 18 and Table III. The data presented in Fig. 18 pertains to 1 cm^3 of material.

Sanitized Copy Approved for Release 2011/03/07 : CIA-RDP80T00246A014400530001-3

Sanitized Copy Approved for Release 2011/03/07 : CIA-RDP80T00246A014400530001-3

Page Denied

Sanitized Copy Approved for Release 2011/03/07 : CIA-RDP80T00246A014400530001-3

Sanitized Copy Approved for Release 2011/03/07 : CIA-RDP80T00246A014400530001-3

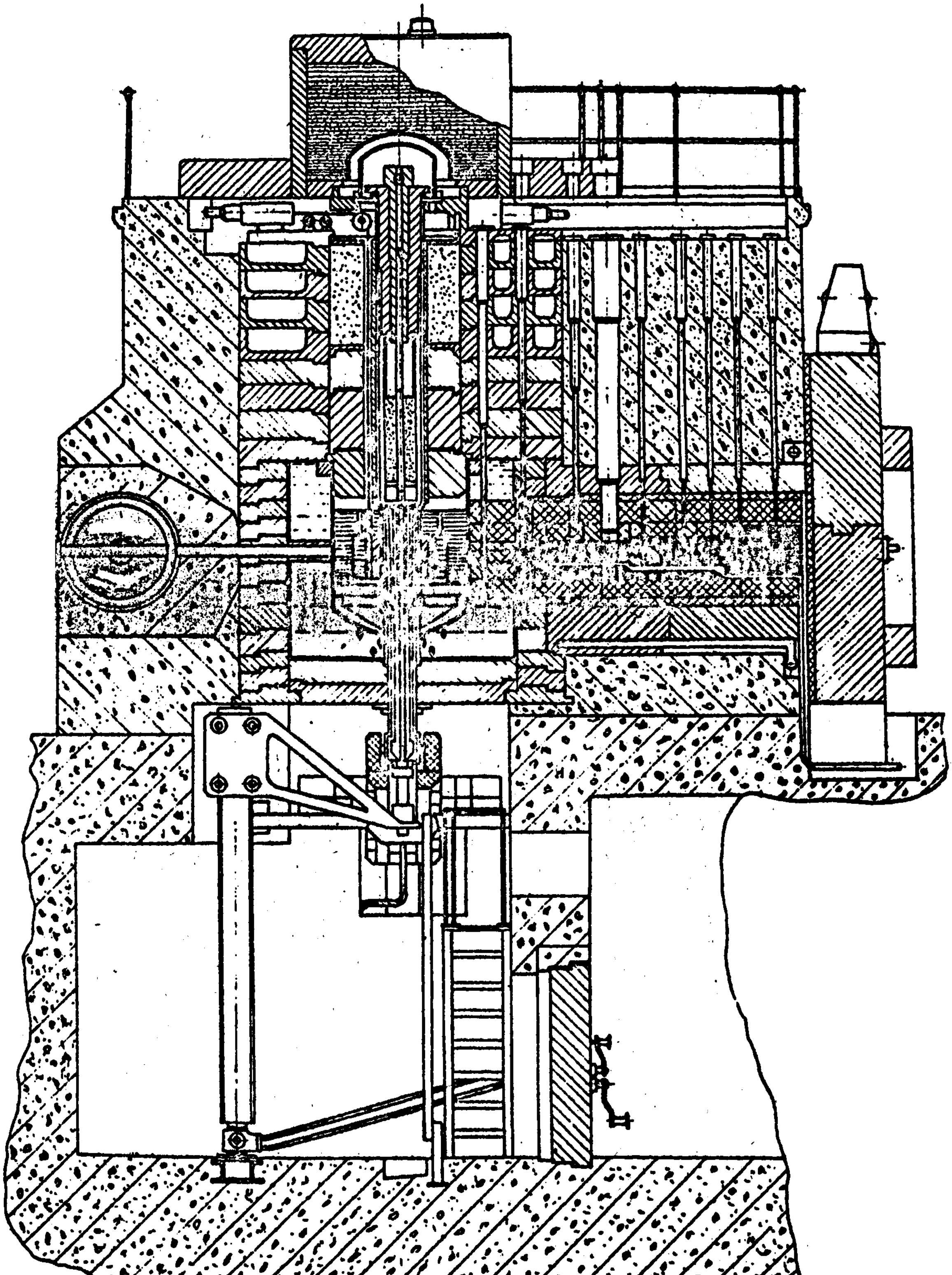

Fig. 1

Vertical Cross-section of Reactor BR-V

Sanitized Copy Approved for Release 2011/03/07 : CIA-RDP80T00246A014400530001-3

Sanitized Copy Approved for Release 2011/03/07 : CIA-RDP80T00246A014400530001-3

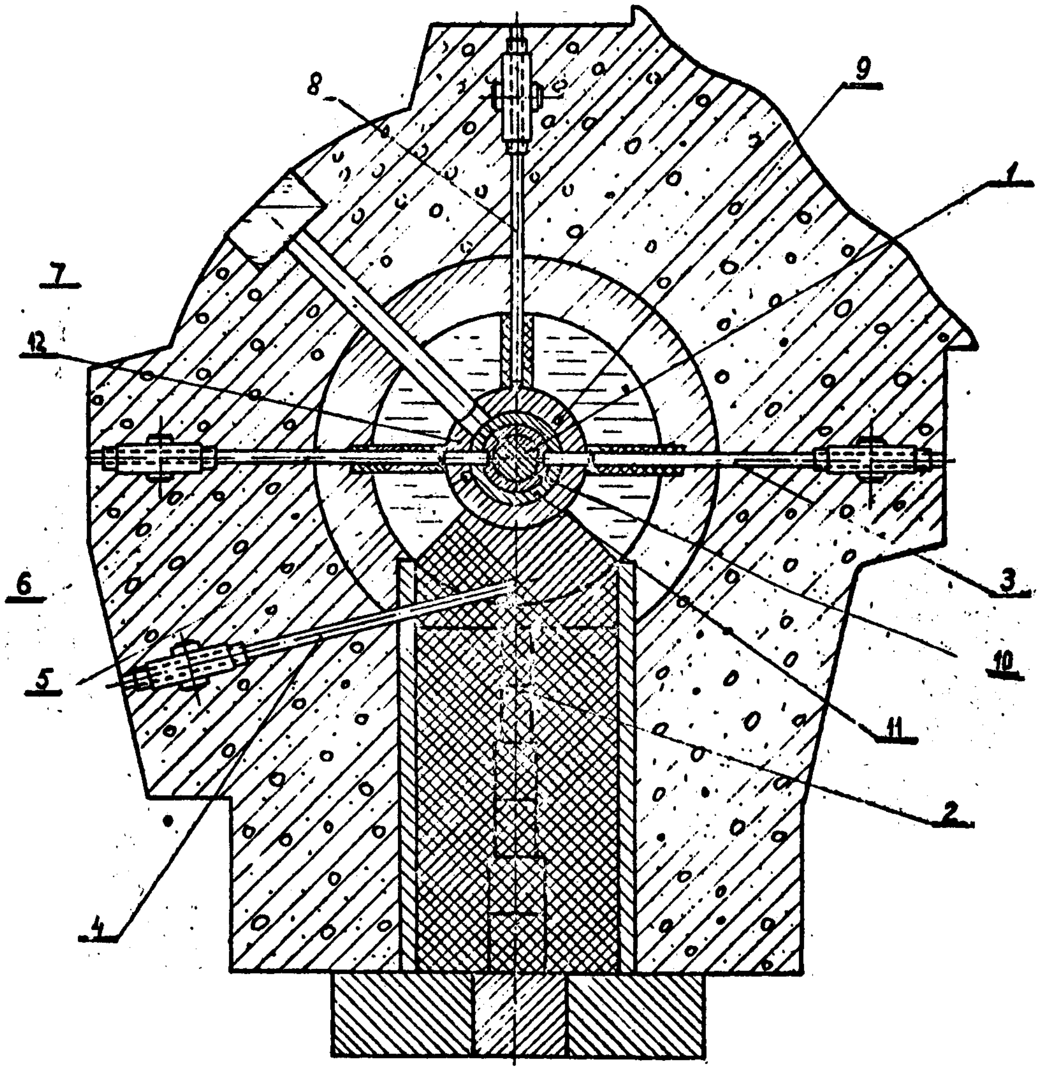

Fig. 2 - Horizontal Cross-section of Reactor BR-V

1 - Core
2 - Channel part of Thermal Column
3 - Channel B-1
4 - Channel T-4
5 - Channel OK-70
6 - Channel B-2
7 - Channel B-2
8 - Channel O-2
9 - Channel OK-50
10 - Compensating Cylinder
11 - Reflector Compensator
12 - Immovable Ni Reflector

Sanitized Copy Approved for Release 2011/03/07 : CIA-RDP80T00246A014400530001-3

Sanitized Copy Approved for Release 2011/03/07 : CIA-RDP80T00246A014400530001-3

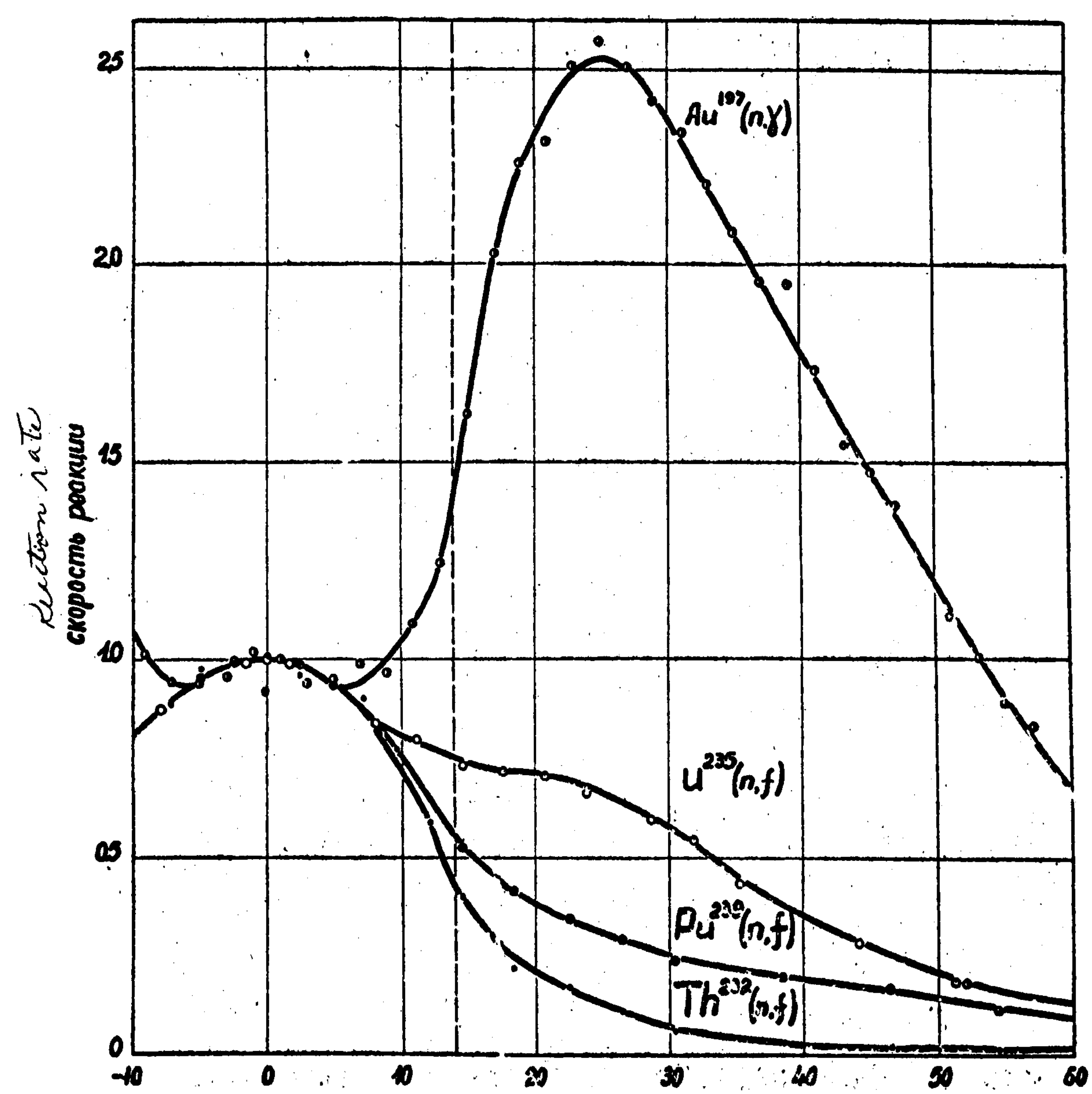

Distance From Center of Core.

Fig. 3

Distribution of rate of different reactions along the central channel of Reactor BR-V. The rate of all reactions in the center of the core is assumed to be unity.

Sanitized Copy Approved for Release 2011/03/07 : CIA-RDP80T00246A014400530001-3

Sanitized Copy Approved for Release 2011/03/07 : CIA-RDP80T00246A014400530001-3

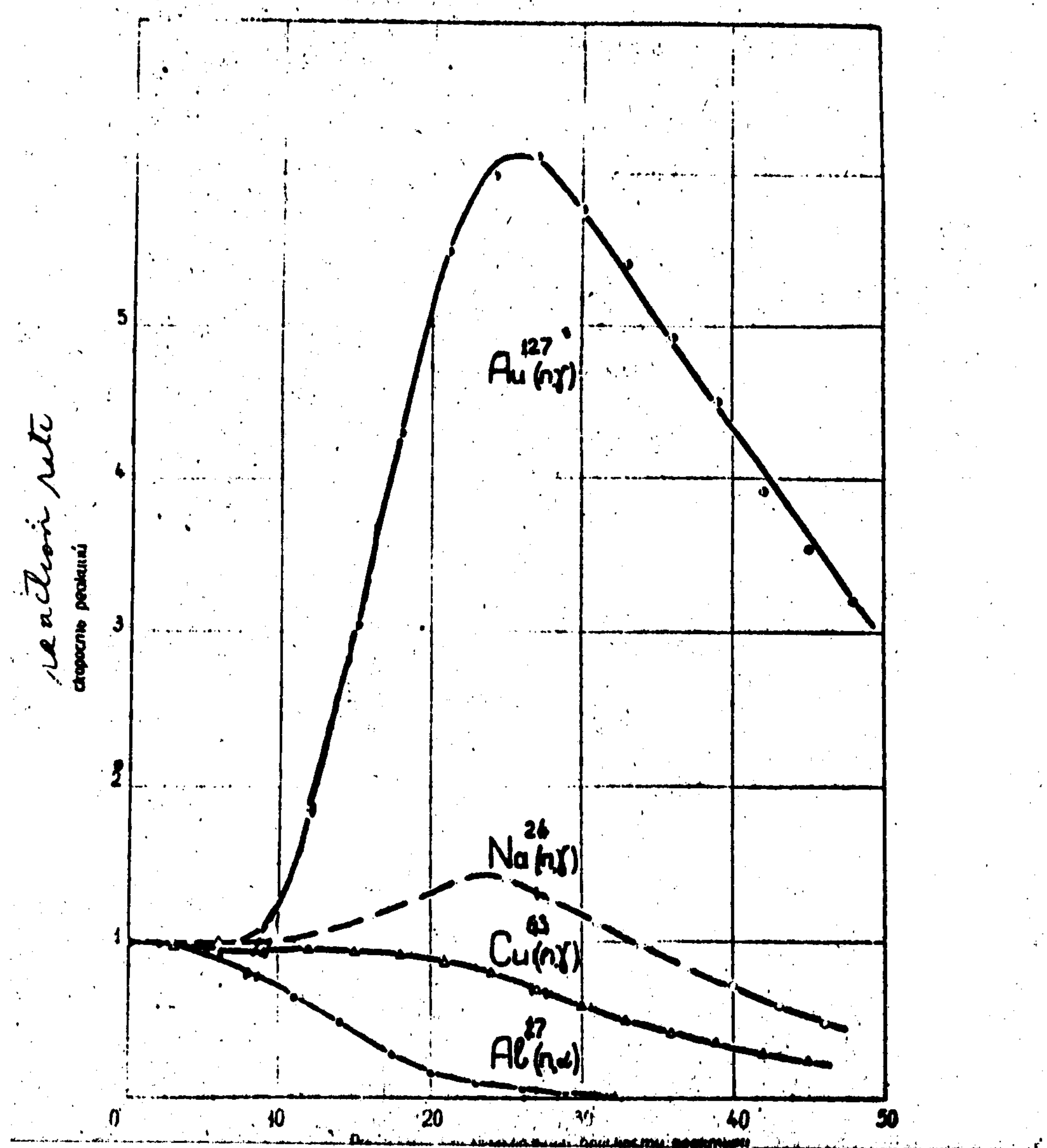

Fig. 4

Distribution of the number of reactions Al(n,α) and of capture in Na^{23}, Cu^{63}, Au^{197} (thin foil), measured in the vertical channel located 5 cm from the center of the reactor. The number of reactions in the antral plane of the core is assumed to be unity.

Sanitized Copy Approved for Release 2011/03/07 : CIA-RDP80T00246A014400530001-3

Sanitized Copy Approved for Release 2011/03/07 : CIA-RDP80T00246A014400530001-3

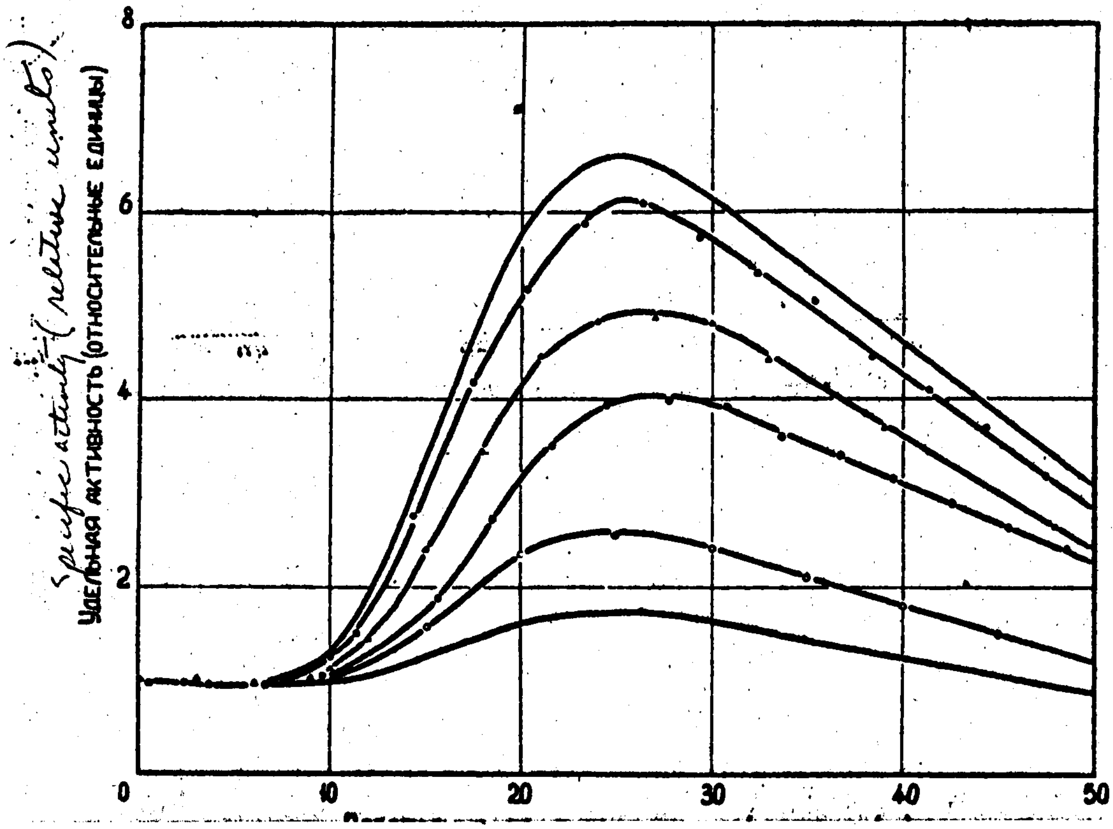

Distance From Center of Core

Fig. 5

Distributions of specific activity of indicators without and with filters of various thicknesses.

● - Indicator thickness 1.35 mg/cm^2 without filter,

△,◐ - Same filter with filters 3.15 and 6.3 mg/cm^2 resp.

O - Indicator thickness 200 mg/cm^2.

The upper curve shows specific activity for ideally thin foil. The lowest one was obtained by extrapolation to infinite filter thickness and represents the unblocked part of activity. All of the foils and filters used were thin relative to energies outside resonances.

Sanitized Copy Approved for Release 2011/03/07 : CIA-RDP80T00246A014400530001-3

Sanitized Copy Approved for Release 2011/03/07 : CIA-RDP80T00246A014400530001-3

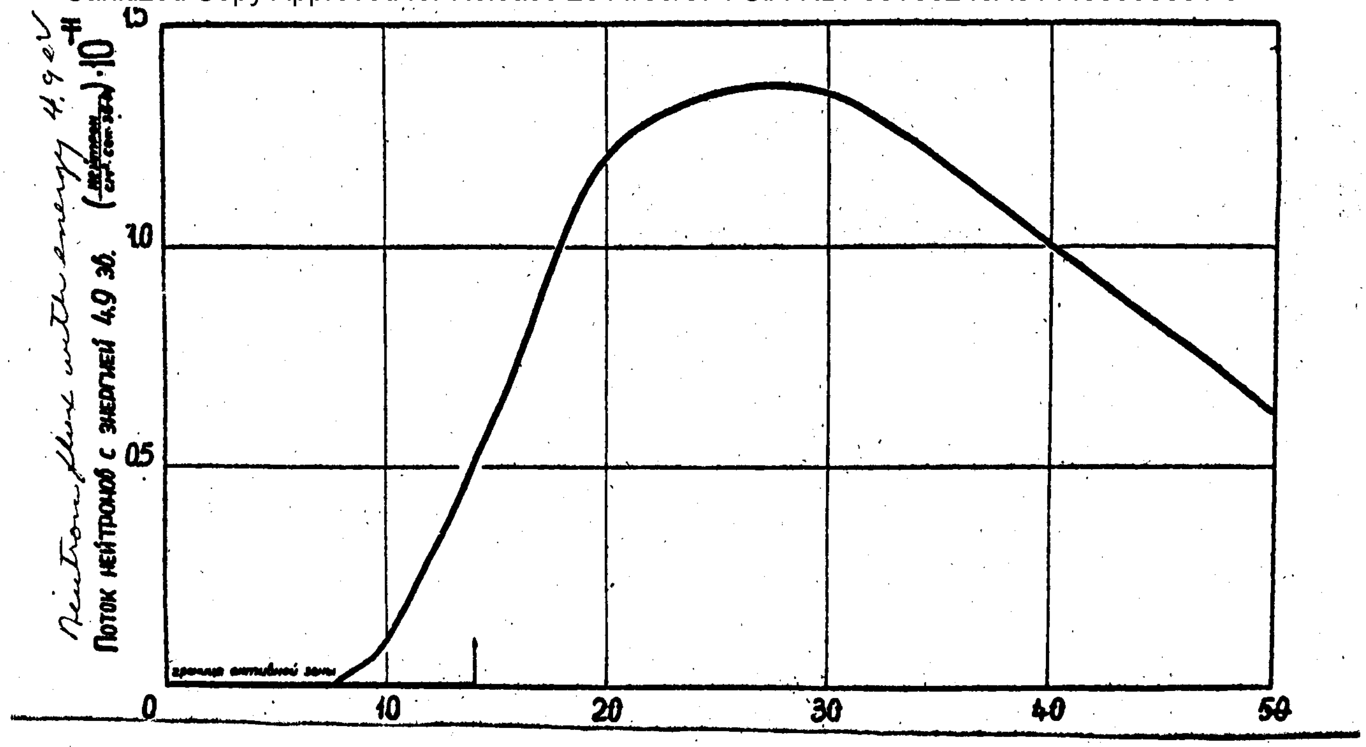

Distance From Center of Core

Fig. 6.

Spacial distribution of neutron flux with En = 4.9 ev along the experimental channel.

Сечения различных реакций в центре активной зоны
σ for different reactions in the center of the core

Реакция	Эксперимент (Expriment)		Расчет (Calculation)
	σ/σ_f (Pu^{239})	σ /барны/ (barns)	σ /барны/
Pu -239 (n,f)	1	1,81	1,81
U -235 (n,f)	0,82±0,03	1,48±0,06	1,46
U -238 (n,f)	0,090±0,004	0,163±0,007	0,16
Au -197 (n,γ)	0,121±0,005	0,22±0,01	0,21

Sanitized Copy Approved for Release 2011/03/07 : CIA-RDP80T00246A014400530001-3

Sanitized Copy Approved for Release 2011/03/07 : CIA-RDP80T00246A014400530001-3

Таблица II

n flux in core & experimental facilities

Потоки нейтронов в активной зоне и экспериментальных устройствах

of reactor BR-5

реактора БР-5 /нейтр./ $см^2$ сек /

	Тепловые Slow	Резонансные /на один log. интервал/ Resonance (in 1 log interval)	Быстрые /выше 1,4 Мэв/ Fast (above 1.4 MeV)	Суммарный поток Total flux
core Центр активной зоны	0	0	$/2,4\pm0,2/10^{14}$	$/8,2\pm0,3/10^{14}$
beam Пучок Б-1 и Б-3	0	0	$/2,2\pm0,2/10^{9}$	$/3,0\pm0,2/10^{10}$
Пучок П-2	0	-	$/1,2\pm0,4/10^{8}$	-
Пучок Т-4	$/8,5\pm0,5/10^{7}$	$/3,4\pm0,5/10^{6}$	$/1,0\pm0,3/10^{6}$	-
maximum neutron Максимальный поток нейтронов в тепловой колонке flux in the thermal column	$/5\pm2/10^{12}$	-	-	-

Sanitized Copy Approved for Release 2011/03/07 : CIA-RDP80T00246A014400530001-3

Sanitized Copy Approved for Release 2011/03/07 : CIA-RDP80T00246A014400530001-3

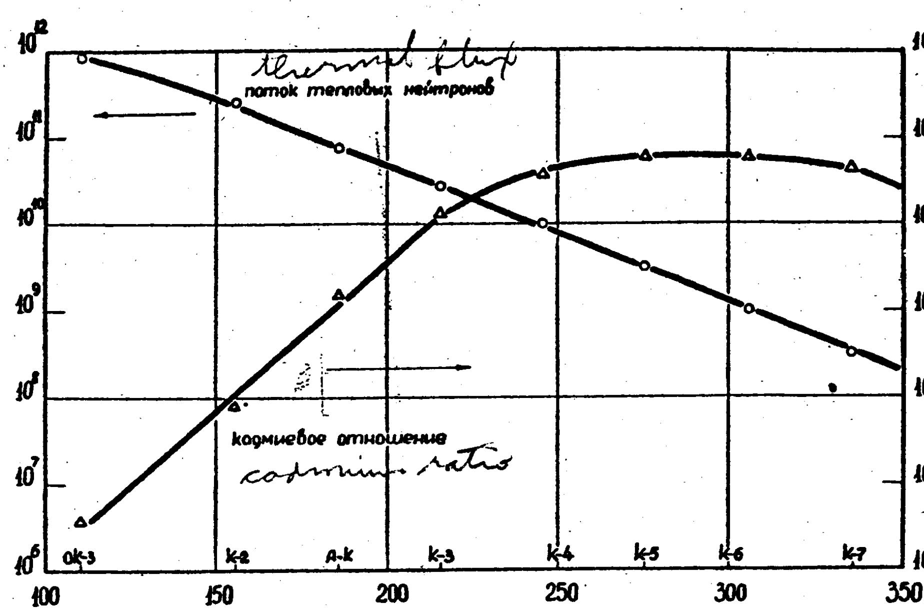

Distance From Center of Reactor

Fig. 7

Distribution of flux of slow neutron along thermal column.

Sanitized Copy Approved for Release 2011/03/07 : CIA-RDP80T00246A014400530001-3

Sanitized Copy Approved for Release 2011/03/07 : CIA-RDP80T00246A014400530001-3

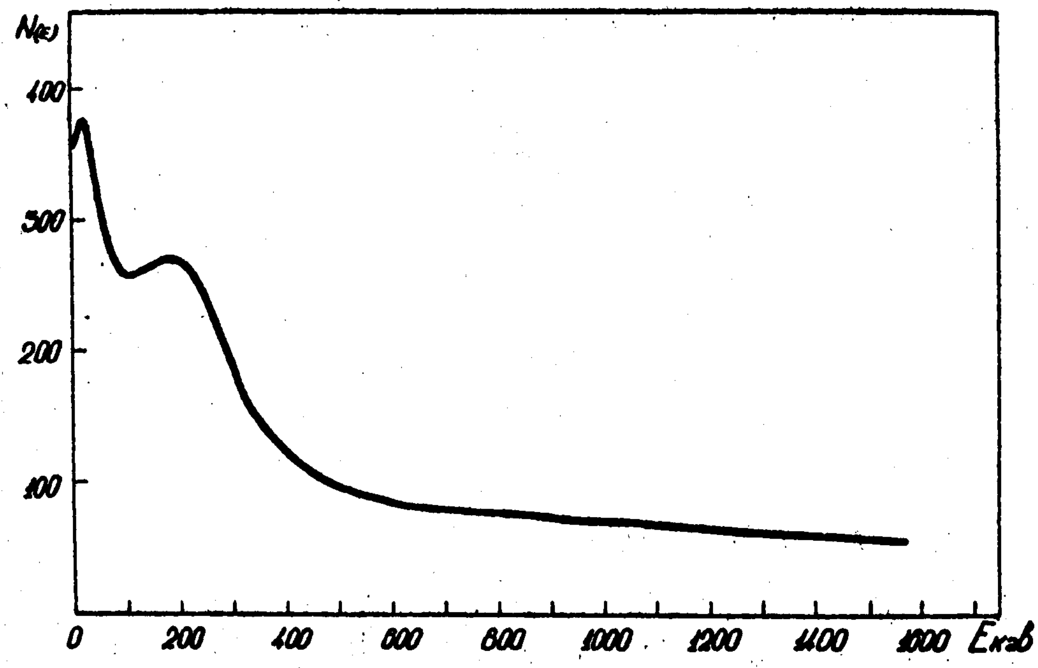

Fig. 8

Spectrum of neutrons in beam B-3. Measurements made by the method of passing neutrons through H-containing medium (n - hexane).

Sanitized Copy Approved for Release 2011/03/07 : CIA-RDP80T00246A014400530001-3

Sanitized Copy Approved for Release 2011/03/07 : CIA-RDP80T00246A014400530001-3

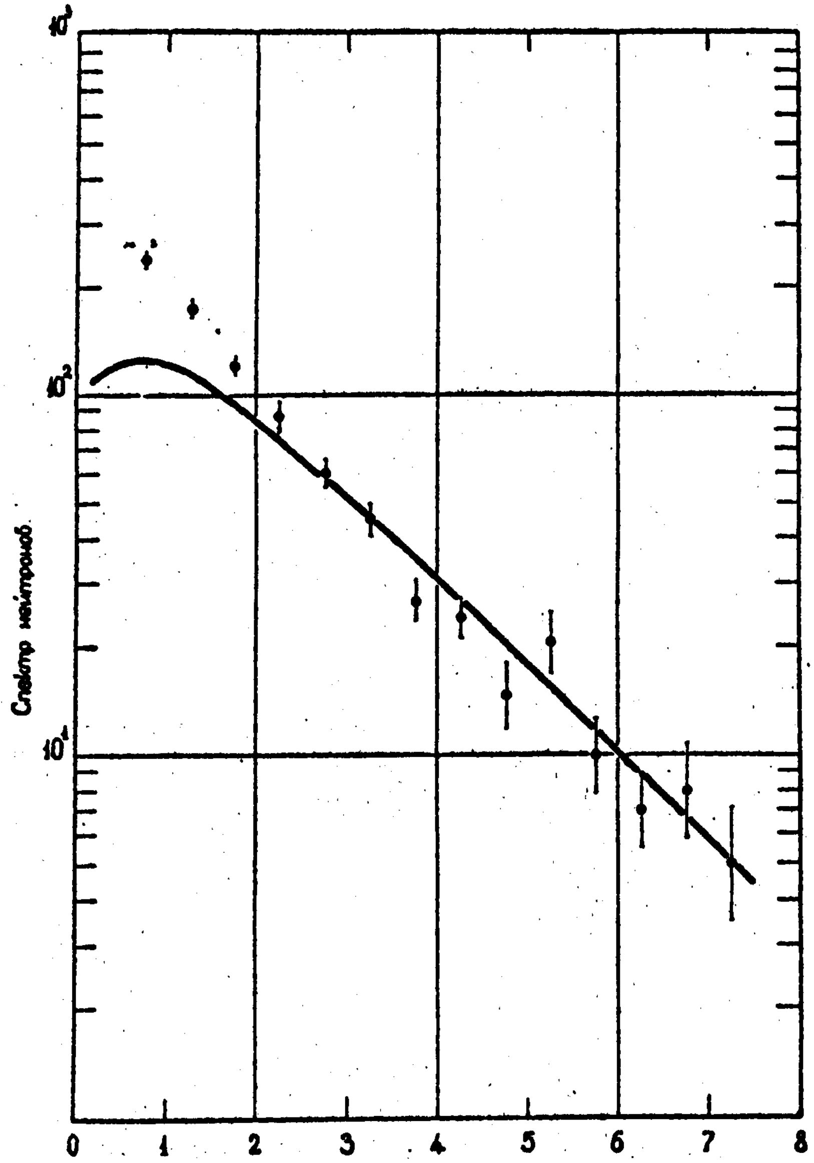

Fig. 9

Hard part of spectrum of neutrons, coming from core measured by method of photo emulsions. Experimental data compared with computed curve

$$\sqrt{En}\; e^{-En/\theta} \qquad \theta = 1.44 \text{ Mev.}$$

for spectrum of instantaneous neutrons of fission of Pu-239.

Sanitized Copy Approved for Release 2011/03/07 : CIA-RDP80T00246A014400530001-3

Sanitized Copy Approved for Release 2011/03/07 : CIA-RDP80T00246A014400530001-3

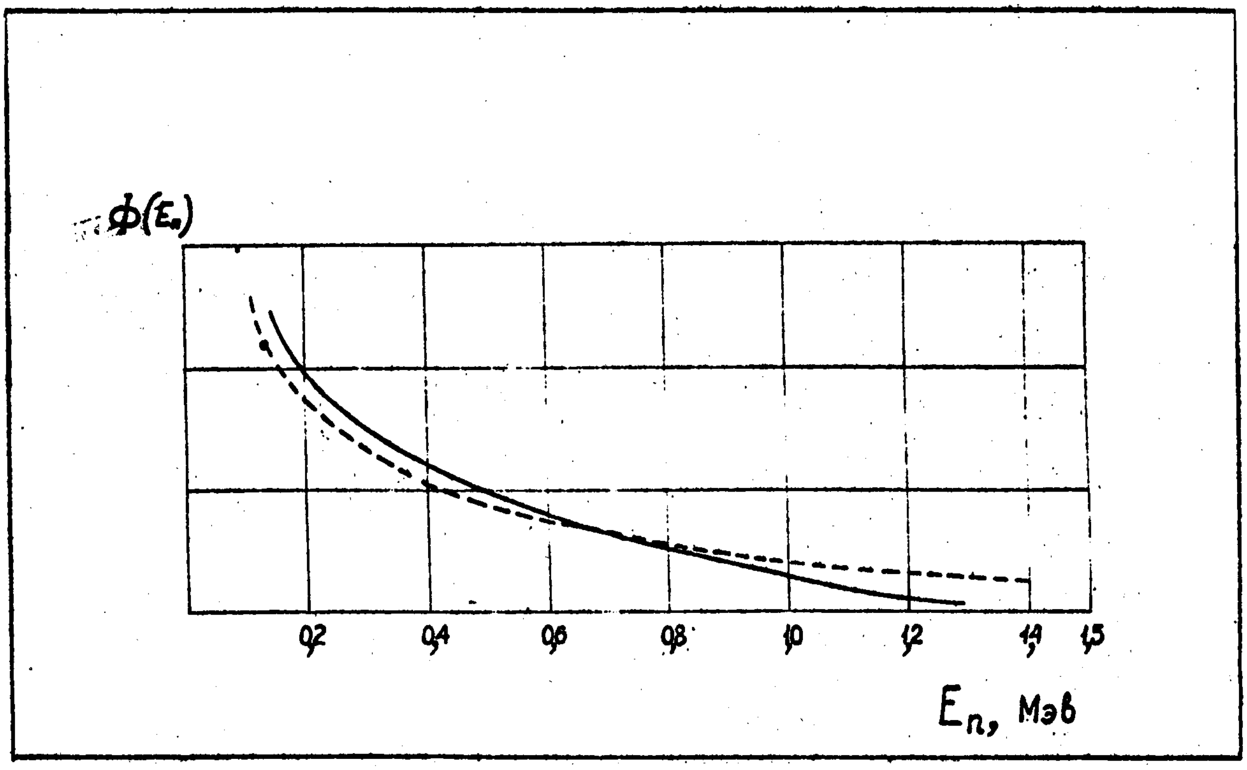

Fig. 10

Neutrons - Spectrum in Channel OK-70. Dotted Curve-Computed.

Sanitized Copy Approved for Release 2011/03/07 : CIA-RDP80T00246A014400530001-3

Sanitized Copy Approved for Release 2011/03/07 : CIA-RDP80T00246A014400530001-3

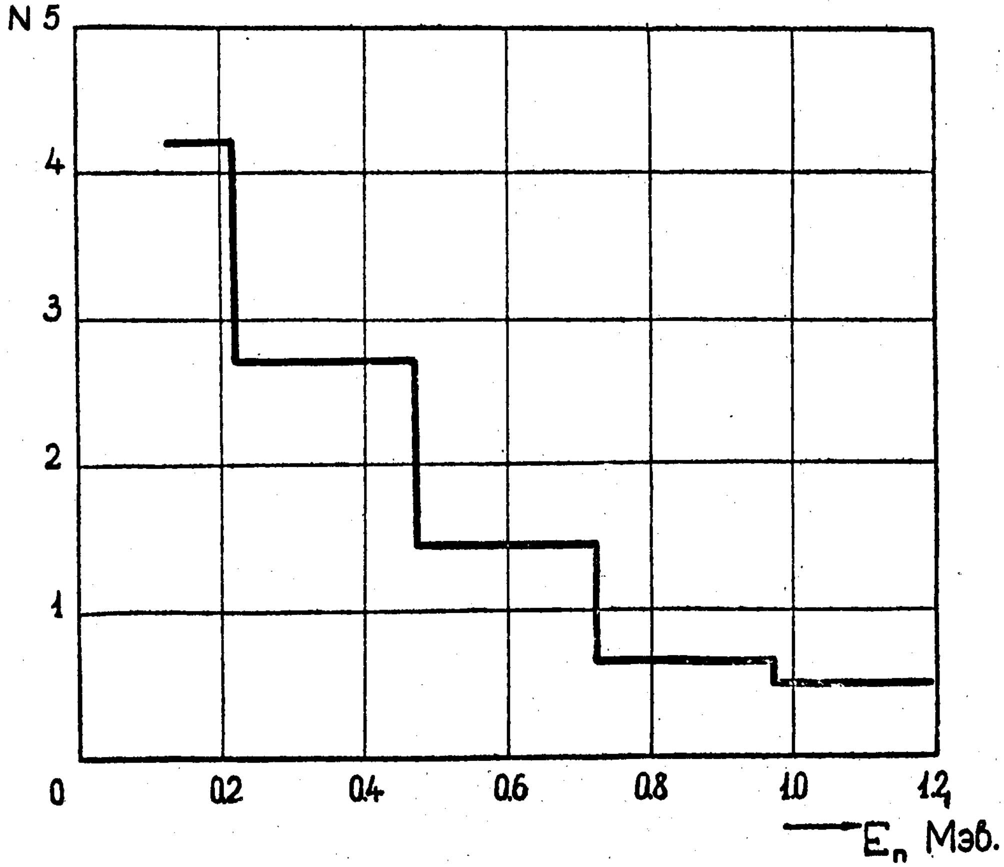

Fig. I1

Computed Neutron Spectrum in Center of Core.

Sanitized Copy Approved for Release 2011/03/07 : CIA-RDP80T00246A014400530001-3

Sanitized Copy Approved for Release 2011/03/07 : CIA-RDP80T00246A014400530001-3

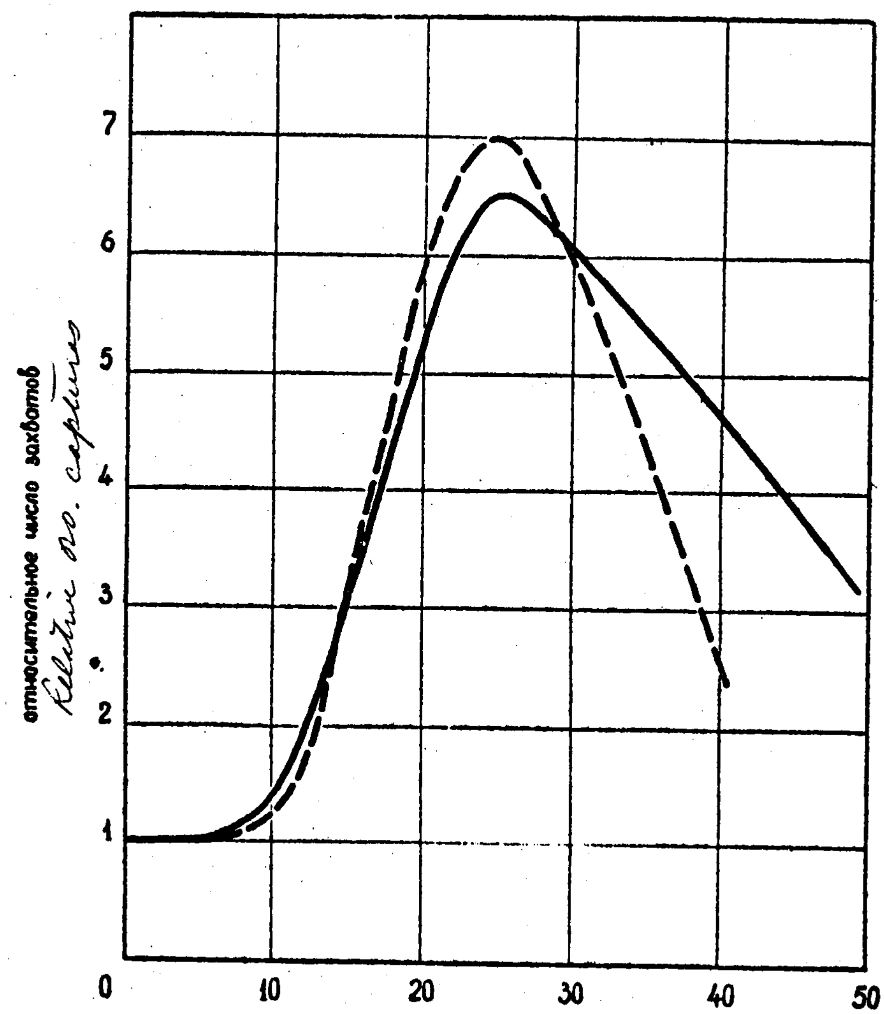

Distance From Central Plane of Reactor

Fig. 12

Comparison of Exp. and Cal. curves of Activation of Au. Solid Curve - Experimental, Dotted - Computed.

Sanitized Copy Approved for Release 2011/03/07 : CIA-RDP80T00246A014400530001-3

Sanitized Copy Approved for Release 2011/03/07 : CIA-RDP80T00246A014400530001-3

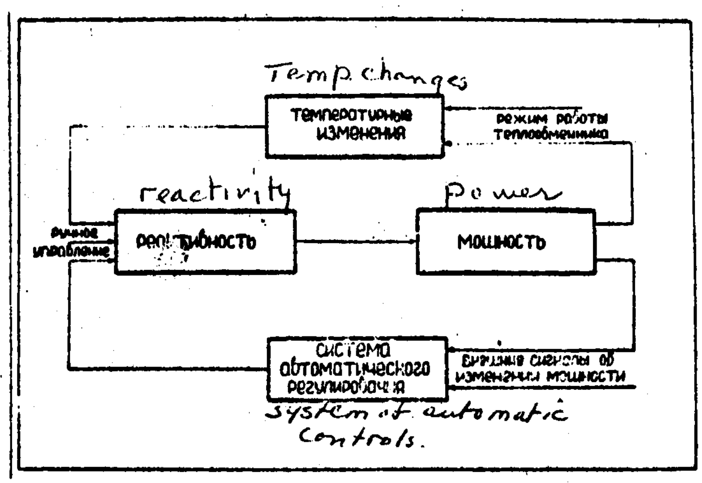

Рис. 13.

(Fig. 13)

61 3866

Sanitized Copy Approved for Release 2011/03/07 : CIA-RDP80T00246A014400530001-3

Sanitized Copy Approved for Release 2011/03/07 : CIA-RDP80T00246A014400530001-3

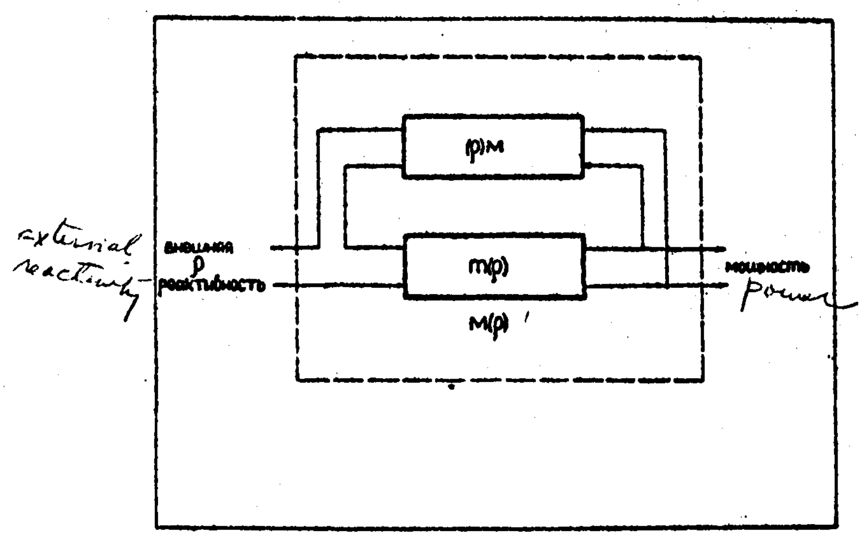

Рис. 14.

(Fig. 14)

61 3868

Sanitized Copy Approved for Release 2011/03/07 : CIA-RDP80T00246A014400530001-3

Sanitized Copy Approved for Release 2011/03/07 : CIA-RDP80T00246A014400530001-3

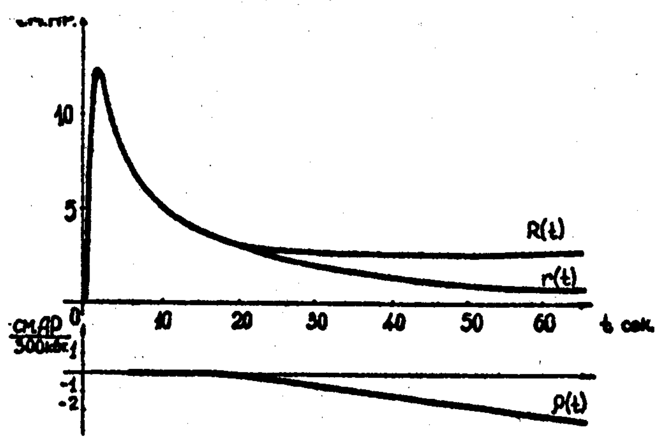

Fig. 15

Sanitized Copy Approved for Release 2011/03/07 : CIA-RDP80T00246A014400530001-3

Sanitized Copy Approved for Release 2011/03/07 : CIA-RDP80T00246A014400530001-3

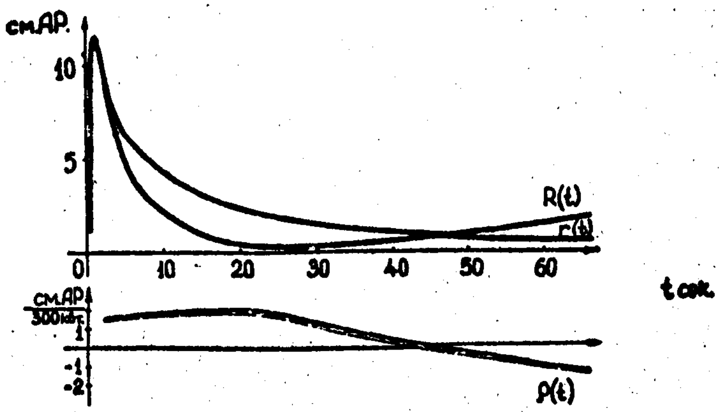

Рис. 16

(Fig. 16)

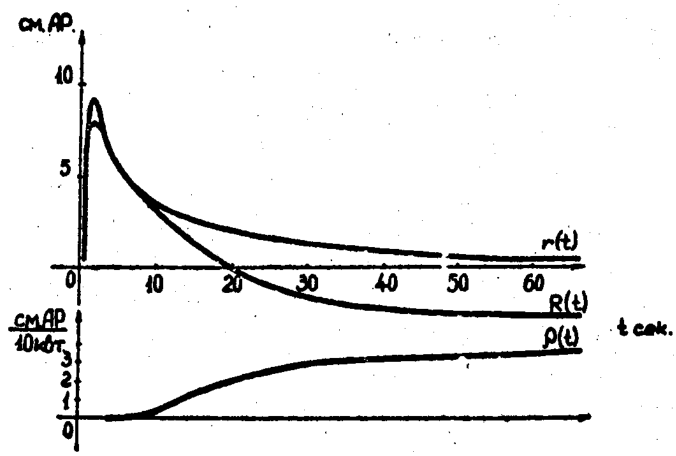

Рис. 17

(Fig. 17)

61 3868

Sanitized Copy Approved for Release 2011/03/07 : CIA-RDP80T00246A014400530001-3

Sanitized Copy Approved for Release 2011/03/07 : CIA-RDP80T00246A014400530001-3

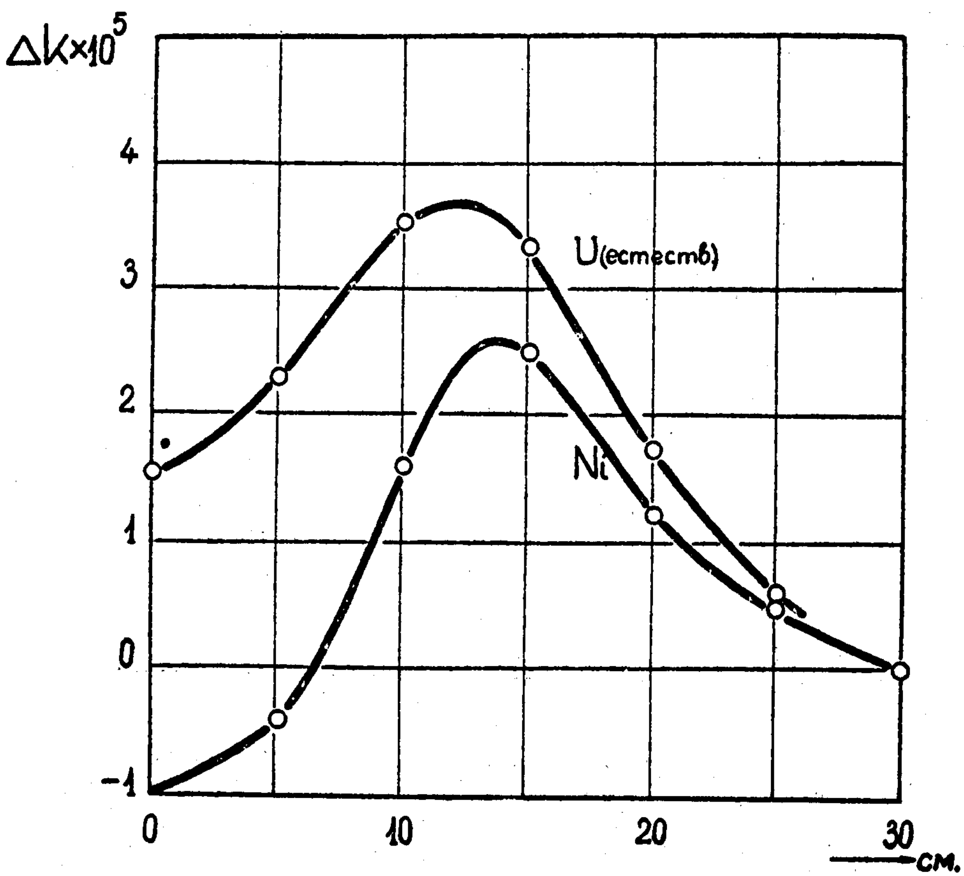

Fig. 18

Change of reactivity when a sample is moved thru the central channel of reactor.

Sanitized Copy Approved for Release 2011/03/07 : CIA-RDP80T00246A014400530001-3